CIRP Increases ICAM-1+ Phenotype of Neutrophils Exhibiting Elevated iNOS and NETs in Sepsis

Yasumasa Ode[1], **Monowar Aziz**[1], and **Ping Wang**[1,2]

[1]Center for Immunology and Inflammation The Feinstein Institute for Medical Research, Manhasset, New York

[2]Department of Surgery and Molecular Medicine, Donald and Barbara Zucker School of Medicine at Hofstra/Northwell, Manhasset, New York

Abstract

Sepsis represents uncontrolled inflammation due to an infection. Cold-inducible RNA-binding protein (CIRP) is a stress-induced damage-associated molecular pattern (DAMP). A subset of neutrophils expressing intercellular adhesion molecule-1 (ICAM-1+ neutrophils) was previously shown to produce high levels of reactive oxygen species. The role of CIRP for the development and function of ICAM-1+ neutrophils during sepsis is unknown. We hypothesize that CIRP induces ICAM-1 expression in neutrophils causing injury to the lungs during sepsis. Using a mouse model of cecal ligation and puncture (CLP)-induced sepsis, we found increased expression of CIRP and higher frequencies and numbers of ICAM-1+ neutrophils in the lungs. Conversely, the CIRP$^{-/-}$ mice showed significant inhibition in the frequencies and numbers of ICAM-1+ neutrophils in the lungs as compared to WT mice in sepsis. *In vitro* treatment of bone marrow-derived neutrophils (BMDN) with recombinant murine CIRP (rmCIRP) significantly increased ICAM-1+ phenotype in a time- and dose-dependent manner. The effect of rmCIRP on increasing frequencies of ICAM-1+ neutrophils was significantly attenuated in BMDN treated with anti-TLR4 Ab or NF-κB inhibitor as compared, respectively, with BMDN treated with isotype IgG or DMSO. The frequencies of inducible nitric oxide synthase (iNOS) producing and neutrophil extracellular traps (NETs) forming phenotypes in rmCIRP-treated ICAM-1+ BMDN were significantly higher than those in ICAM-1− BMDN. Following sepsis the ICAM-1+ neutrophils in the lungs showed significantly higher levels of iNOS and NETs compared to ICAM-1− neutrophils. We further revealed that ICAM-1 and NETs were co-localized in the neutrophils treated with rmCIRP. CIRP$^{-/-}$ mice showed significant improvement in their survival outcome (78% survival) over that of WT mice (48% survival) in sepsis. Thus, CIRP could be a novel therapeutic target for regulating iNOS producing and NETs forming ICAM-1+ neutrophils in the lungs during sepsis.

Correspondence address: Ping Wang, MD, Head, Center for Immunology and Inflammation, The Feinstein Institute for Medical Research, Professor of Surgery and Molecular Medicine, Donald and Barbara Zucker School of Medicine at Hofstra/Northwell, 350 Community Drive, Manhasset, NY 11030, Tel: (516) 562-3411, Fax: (516) 562-2396, pwang@northwell.edu.

Conflict of Interest Disclosure
The authors report no financial conflicts of interest

Summary sentence:

Our findings involving CIRP, ICAM-1^{+} neutrophils and NETs implicate a novel pathophysiology of sepsis-induced acute lung injury, and targeting CIRP could be an effective therapeutic tool to control sepsis-induced acute lung injury.

Keywords

CIRP; Sepsis; Lung; Neutrophil; ICAM-1; NETs; iNOS

INTRODUCTION

Sepsis is defined as life-threatening organ dysfunction caused by a dysregulated host response to infection [1]. A recent survey estimated its annual global incidence at 31.5 million cases, resulting in 5.3 million deaths [2]. Sepsis is often complicated by acute lung injury (ALI), clinically defined as acute respiratory distress syndrome (ARDS) [3]. ALI is developed as a consequence of excessive neutrophil infiltration and pulmonary endothelial cell (EC) activation by microbial pathogen-associated molecular patterns (PAMPs) or endogenous damage-associated molecular patterns (DAMPs) [4–6]. A clear understanding of the ALI pathophysiology with respect to the novel phenotypes and functions of neutrophils will help develop effective therapeutic potential against this deadly clinical condition.

Cold-inducible RNA-binding protein (CIRP) is a glycine-rich RNA chaperone facilitating RNA translation [7]. Mouse and human CIRP contain 172 amino-acid residues, which share 95% sequence similarity [7]. Patients with hemorrhagic shock have increased levels of CIRP in the blood [8]. Similarly, in animal models of hemorrhage and sepsis, CIRP is released into the circulation and serves as a DAMP to induce the release of pro-inflammatory cytokines and causes EC dysfunction [8]. The role of CIRP in macrophages, lymphocytes and ECs has been demonstrated [8–11], while the direct role of CIRP on neutrophils during sepsis is unknown.

Neutrophils play an essential role in the innate immune response, providing a first line of host defense. Neutrophils can trap and kill microorganisms by releasing neutrophil extracellular traps (NETs) composed of chromatin and antimicrobial proteins [12–14]. Conversely, the NETs and their components contributing to the pathogenesis of sepsis and other inflammatory diseases have also been reported [14, 15]. Alterations in the phenotypes of neutrophils may influence to their activation and functions. Therefore, elucidation of the novel phenotypes of neutrophils during sepsis will rewrite the pathophysiological features of ARDS.

Intercellular adhesion molecule-1 (ICAM-1), also known as CD54 is a member of the immunoglobulin (Ig)-like gene superfamily [16]. ICAM-1 is predominantly expressed on the endothelial and epithelial cells and to a lesser extent on certain subsets of leukocytes [17, 18]. Its expression is up-regulated by the stimulation with lipopolysaccharide (LPS), tumor necrosis factor-α (TNF-α), interleukin (IL)-1β and interferon (IFN) γ [17–19]. ICAM-1

plays pivotal role in cell adhesion, migration and aggregation via the interactions with its ligands, the integrins such as leukocyte function-associated antigen-1 (LFA-1) and Mac-1 [20–23]. With respect to neutrophils, little is known about the status of ICAM-1 expression. An increased expression of ICAM-1 on neutrophils after stimulation with LPS and TNF-α has been shown, which resulted in significant increases in neutrophil-neutrophil adherence and aggregation [24]. The ICAM-1 expressing neutrophils were shown to enhance the effector functions through the increase of phagocytosis and ROS generation [25]. The role of this subset of neutrophils in terms of augmenting inflammation and tissue injury in a clinically relevant model of systemic inflammation has not been reported so far.

Although the effect of LPS and pro-inflammatory cytokines to induce ICAM-1 expression in neutrophils has been demonstrated [24, 25], the role of DAMPs on ICAM-1 expression in neutrophils is unknown. We have recently identified CIRP to act as a novel DAMP which exaggerates inflammation [8]. Elucidation of the role of CIRP on neutrophils for the expression of ICAM-1 will provide crucial information for developing novel therapeutic potential. Thus, we hypothesized that CIRP could induce ICAM-1 expression on neutrophils through binding to its receptor Toll-like receptor 4 (TLR4), leading to exaggerated inflammation and lung injury during sepsis.

We noticed that expression of CIRP and the numbers of ICAM-1$^+$ neutrophils were both upregulated in lungs during sepsis. Using CIRP knock-out (CIRP$^{-/-}$) mice we showed a decreased content of ICAM-1$^+$ population of neutrophils in lungs during sepsis. We also revealed the mechanism of CIRP-induced ICAM-1 expression in neutrophils through the involvement of TLR4/nuclear factor (NF)-κB-mediated pathway. Finally, we identified pro-inflammatory function of ICAM-1$^+$ neutrophils in terms of their ability to produce higher levels of inducible nitric oxide synthase (iNOS) and NETs. Collectively, these findings clearly revealed a unique role of CIRP on neutrophils to cause exaggerated inflammation and ARDS in sepsis. Thus, targeting CIRP could be an effective therapeutic potential to reduce ICAM-1$^+$ population of neutrophils in lungs thereby ameliorating sepsis-induced ARDS.

MATERIALS AND METHODS

Mice

Male 8–9 week old wild-type (WT) C57BL/6 mice weighing about 25 g were purchased from Charles River (Charles River, Wilmington, MA). C57BL/6 background CIRP$^{-/-}$ mice were obtained as a gift from Dr. Fujita (Kyoto University, Kyoto, Japan). Mice were housed in temperature-controlled rooms with 12 h light cycles and fed standard laboratory chow and water ad libitum. All experiments were performed in accordance with the guidelines for the use of experimental animals by National Institutes of Health (Bethesda, MD). All the animal experimental protocols were approved by the Institutional Animal Care and Use Committees (IACUC) of the Feinstein Institute for Medical Research.

Cecal ligation and puncture (CLP)-induced sepsis

WT and CIRP$^{-/-}$ mice were anesthetized with 2% isoflurane inhalation. The abdomen was shaved and made sterile with 10% povidone-iodine swab. CLP was performed as described previously [26]. Briefly, after a 1.5 cm midline abdominal incision the cecum was exposed and ligated at 1 cm from the tip with 4–0 silk suture. Ligated distal part of the cecum was punctured once through and through using a 22-g needle and squeezed gently to extrude a small amount of fecal material. The cecum was positioned back inside the abdomen, and the abdominal wound was closed in two layers with running 4–0 silk suture. Sham mice underwent only abdominal incision without ligation and puncture of the cecum. Both sham- and CLP-operated animals were resuscitated with 1 ml of normal saline subcutaneously, and then returned to their cages with normal access to foods and drinking water for 20 h.

Assessment of CIRP expression in lung by Western blot

After 20 h of sham or CLP operation, lungs were harvested from each animal and homogenized in lysis buffer containing 10 mM Tris-HCl, pH 7.5, 120 mM NaCl, 1% NP-40, 1% sodium deoxycholate and 0.1% sodium dodecyl sulfate and protease inhibitor cocktail (Roche Diagnostics, Indianapolis, IN) by sonication (Sonic Dismembranator 100; Fisher Scientific, Pittsburgh, PA). Concentration of protein of each sample was determined by Bio-Rad protein assay reagent (Bio-Rad, Hercules, CA). Equal amounts of lung homogenates were fractionated on Bis-Tris gels (4–12%) and transferred to 0.2 μm pore size nitrocellulose membrane. The membrane was blocked with 0.1% casein in Tris-buffered saline with 0.1% tween-20 (TBST) and incubated with anti-mouse CIRP Ab (Cat. No.: 10209–2-AP; Proteintech, Rosemont, IL) or β-actin primary Ab (Cat. No.: A5441; Sigma-Aldrich, St Louis, MO). After washing the membranes with TBST buffer, they were incubated with fluorescent-labeled secondary Abs (Li-Cor Biosciences, Lincoln, NE). Bands were detected by Odyssey FC Dual-Mode Imaging system (Li-Cor Biosciences), and the intensities of bands were measured using Image J software [27].

Isolation of cells from lung tissues

Lung tissues were sliced into small pieces by sterile surgical blade and suspended in Ca^{++} and Mg^{++} free Hank's balanced salt solution (HBSS, Corning, NY). Tissue digestion was performed in HBSS supplemented with 100 U/ml of collagenase I (Worthington Biochemical, Lakewood, NJ) and 20 U/ml DNase I (Worthington Biochemical, Lakewood, NJ) in 37°C water bath for 30 min with periodic shaking. Digested tissue fragments were crushed with a 10 ml syringe plunger and passed through a 70 μm cell strainer (Corning). Lysis of red blood cells in lung cell suspensions was done using ACK lysis buffer (Mediatec, Manassas, VA). The numbers of isolated lung cells were counted using a microscope (Eclipse TS100; Nikon, Tokyo, Japan).

Isolation and purification of bone marrow-derived neutrophils (BMDN)

Mice were anesthetized by 2% isoflurane inhalation and the femurs and tibias were dissected. Marrow contents form bones were flushed out with Ca^{++} and Mg^{++} free HBSS using a 25 gauge needle into a petri dish. Suspensions of cells were filtered through a 70 μm cell strainer (Corning) and BMDN were purified by negative selection using the EasySep

mouse neutrophil enrichment kit (Cat. No.: 19762; STEMCELL, Vancouver, BC, Canada). The purity of the sorted neutrophils was assessed by staining the cells with APC-Ly6G Ab (clone 1A8; Biolegend, San Diego, CA) using BD LSR Fortessa flow cytometer (BD Biosciences, San Jose, CA).

Assessment of ICAM-1 expression in neutrophils by real-time PCR and Western blot

Total RNA was extracted from 2×10^6 BMDN treated with either PBS or rmCIRP (1 μg/ml) for 2 h using TRIzol (Invitrogen; Carlsbad, CA) and reverse-transcribed into cDNA using reverse transcriptase enzyme (Applied Biosystems; Foster City, CA). The PCR reaction was performed in 20 μl of final volume containing 0.08 μM of forward and reverse primer, cDNA, and 10 μl SYBR Green PCR Master Mix (Applied Biosystems). The thermal profile used by the Applied Biosystems 7300 real-time PCR machine was: 50°C for 2 min, 95°C for 10 min, 45 cycles of 95°C for 15 seconds, and 60°C for 1 min. Mouse β-actin served as an internal control gene for normalization. Relative expression of mRNA was represented as fold change in comparison to the sham group. The sense and anti-sense primer sequences of mouse genes include, ICAM-1 (NM_010493): 5'-GGGCTGGCATT GTTCT CTAA-3', 5'-CTTCAGAGGCAGGAAACAGG-3' and β-actin (NM_007393): 5'-CGTGAAA AGATGACCCAGATCA-3' and 5'-TGGTACG ACCAGAGGCATACAG-3'. To assess the protein levels of ICAM-1 expression in neutrophils, a total of 2×10^6 BMDN were treated with rmCIRP at a dose 1 μg/ml for 4 h, and then total proteins were extracted from the BMDN and subjected to Western blot for the determination of ICAM-1 expression by reacting the cell lysates with anti-mouse ICAM-1 Ab (Cat. No.: sc-1511; Santa Cruz Biotechnology, Santa Cruz, CA) or anti-β-actin primary Ab (Cat. No.: A5441; Sigma-Aldrich) and detected by Odyssey FC Dual-Mode Imaging system.

Assessment of ICAM-1 expression in neutrophils by flow cytometry

To detect ICAM-1 expression on the surface of neutrophils, a total of 1×10^6 cells isolated from lungs or purified BMDN following CLP or treatment with our in-house made recombinant mouse CIRP (rmCIRP) were washed with fluorescence-activated cell sorting (FACS) buffer containing phosphate buffered saline (PBS) with 2% FBS and stained with APC anti-mouse Ly-6G Ab (clone: 1A8; Biolegend) and FITC anti-mouse ICAM-1 Ab (CD54, clone: 3E2; BD Biosciences, San Jose, CA). Unstained cells were used as a negative control to establish the flow cytometer voltage setting, and single-color positive controls were used for the adjustment of the compensation. Acquisition was performed on 30,000 events using a BD LSR Fortessa flow cytometer (BD Biosciences, San Jose, CA) and data were analyzed with FlowJo software (Tree Star, Ashland, OR). ICAM-1 expressing neutrophils were defined as Ly6G⁺CD54⁺ population.

In vitro study of TLR4 and NF-κB pathways

BMDN were cultured in RPMI medium with 10% heat inactivated fetal bovine serum (FBS) and penicillin and streptomycin and stimulated with rmCIRP at different doses and time points. For inhibition of TLR4, BMDN were pre-treated with a neutralizing Ab against TLR4, anti-mouse TLR4 Ab (clone: MTS510; Biolegend) at a dose of 6 μg/ml or isotype IgG control (clone: RTK2071; Biolegend) at a dose of 6 μg/ml for 30 min, followed by the stimulation with rmCIRP (1 μg/ml) for 4 h. Expression of ICAM-1 in BMDN was then

assessed by flow cytometry. To assess the involvement of NF-κB for ICAM-1 expression, BMDN were pre-treated with either IKK16, a selective inhibitor of IκB kinase (Cat. No.: 2539; Bio-Tech, Minneapolis, MN) at a dose of 0.5 μM or DMSO as vehicle control for 30 min, followed by the stimulation with rmCIRP at 1 μg/ml for 4 h. Expression of ICAM-1 in BMDN was assessed by flow cytometry.

Assessment of iNOS expression by flow cytometry

For the assessment of intracellular iNOS expression, a total of 1×10^6 BMDN in RPMI medium were stimulated with 1 μg/ml rmCIRP for 4 h at 37°C in 5% CO_2 cell culture incubator. Following incubation, the cells were stained with APC anti-mouse Ly-6G Ab (clone: 1A8; Biolegend) and FITC-anti-mouse ICAM-1 Ab (clone: 3E2; BD Biosciences) and then fixed and permeabilized using BD cytofix/cytoperm plus fixation/permeabilization kit (Cat. No.: 554715; BD Biosciences), followed by the intracellular staining with PE-anti-mouse iNOS Ab (Cat. No.: sc-651; Santa Cruz Biotechnology, Santa Cruz, CA). Acquisition was performed on 30,000 events using a BD LSR Fortessa Flow Cytometry Analyzer (BD Biosciences) and data were analyzed by FlowJo software (Tree Star, Ashland, OR).

Assessment of NETs by flow cytometry

To detect NETs using flow cytometry, purified BMDN were stimulated with 500 ng/ml rmCIRP for 4 h at 37°C in 5% CO_2 humidified incubator. After stimulation, neutrophils were fixed with 2% paraformaldehyde for 20 min at room temperature, blocked for 30 min with 2% bovine serum albumin in PBS at 37°C. Without a permeabilization step, the cells were then stained with APC-rat anti-mouse Ly-6G Ab (clone: 1A8; Biolegend), BV421-hamster anti-mouse ICAM-1 Ab (clone: 3E2; BD Bioscience) and with FITC-mouse anti-myeloperoxidase (MPO) Ab (clone: 2D4; Abcam, Cambridge, MA). A total of 30,000 events were acquired using a BD LSR Fortessa Flow Cytometry Analyzer (BD Biosciences) and the data were analyzed by FlowJo software (Tree Star, Ashland, OR).

Assessment of the co-localization of NETs and ICAM-1 on neutrophils by microscopy and imaging flow cytometry

A total of 1×10^5 BMDN grown in culture slides (Cat. No.: 177402; Thermo Fisher Scientific, Waltham, MA) were treated with rmCIRP (1 μg/ml) for 4 h at 37°C. The cells were fixed with 4% paraformaldehyde and then stained with SYTOX green (2μM; Thermo Fisher Scientific) and PE-anti-mouse ICAM-1 Ab (Cat. No.: sc-8439 PE; Santa Cruz Biotechnology), followed by the assessment using fluorescence microscope (Eclipse TS100; Nikon). Purified BMDN (2×10^6) were stimulated with rmCIRP (1 μg/ml) at 37°C for 4 h. Cells were surface stained with FITC MPO (clone: 2D4; Abcam) and PE ICAM-1 (Cat. No.: sc-8439 PE; Santa Cruz Biotechnology) Abs and subjected to acquisition in ImageStreamX Mark II flow cytometer (BD Biosciences) and analysis by INSPIRE and IDEAS software.

Survival study in mouse model of sepsis

WT and CIRP$^{-/-}$ mice were subjected to ligation of cecum at 0.5 cm from the tip with 4–0 silk suture. A single puncture was done to the distal part of the ligated cecum using a 22-gauge needle. A small amount of cecal content was extruded from the punctured cecum.

After wound closure using 4–0 silk suture, the mouse was injected with 500 μl of the antibiotic Imipenem (0.5 μg/kg BW), and 500 μl of normal saline subcutaneously. The animals were followed twice a day up to 10 days.

Statistical analysis

Data are presented as mean ± standard error of the mean (SEM). Differences between two groups were assessed with the unpaired Student's *t* test. The p values < 0.05 were considered statistically significant. Multiple groups were compared by one-way analysis of variance (ANOVA) using the Student-Newman-Keuls test. All statistical tests were performed and graphics were created by using Sigma Plot graphing and statistical analysis software (Systat Software Inc., San Jose, CA).

RESULTS

CIRP expression is increased in the lungs in sepsis

Systemic levels of CIRP were shown to be elevated following sepsis and in other inflammatory diseases in rodents and in humans in the previous studies [8, 28]. However, the status of CIRP expression in the lungs following sepsis was unknown. Here, we assessed the protein levels of CIRP in the lungs which showed significant upregulation at 20 h of CLP by a mean value of 41.7% compared to sham-operated animals (Fig 1A).

The frequencies and numbers of ICAM-1+ neutrophils are increased in sepsis

After 20 h of CLP, whole blood and lung cells were isolated to assess the surface expression of ICAM-1 on neutrophils. In sham-operated mice, mean values of 16.1% and 18.7% neutrophils in the blood and lung tissues were found to be positive for surface expression of ICAM-1, respectively (Fig 1B-E). Interestingly, sepsis resulted in significant induction of the frequencies of ICAM-1 expressing neutrophils to mean values of 35.0% and 31.4% in the blood and lung tissues, respectively (Fig 1B-E). Moreover, the total number of ICAM-1 expressing neutrophils in the lungs was also found to be significantly increased by a mean value of 72% in CLP-operated mice compared to sham-operated mice (Fig 1D, F).

Deficiency of CIRP is associated with decreased contents of ICAM-1+ neutrophils in sepsis

We noticed that CIRP levels and ICAM-1 expressing neutrophils were both increased in sepsis (Fig 1). To reveal the association between CIRP and ICAM-1+ neutrophils, we assessed the expression of ICAM-1 on the surface of neutrophils in the lungs following induction of sepsis in WT and CIRP$^{-/-}$ mice. As shown in Fig 2A-C, after 20 h of sepsis WT and CIRP$^{-/-}$ mice showed significantly higher levels of ICAM-1 expressing neutrophils in the lungs in terms of frequencies and numbers as compared to their respective sham-operated groups. Interestingly, we noticed significant reduction in the frequencies and numbers of ICAM-1 expressing neutrophils in the lungs of septic CIRP$^{-/-}$ mice by mean values of 52.9% (Fig 2A, B) and 38.6% (Fig 2A, C), respectively as compared to WT mice with sepsis. These data clearly shows the link between CIRP and ICAM-1+ neutrophils in lungs during sepsis.

Treatment with rmCIRP induces ICAM-1 expression on neutrophils

We first assessed the expression of ICAM-1 at its mRNA and protein levels in the neutrophils after treatment with rmCIRP by using real-time PCR and Western blot, respectively. We found that the BMDN treated with rmCIRP showed marked up-regulation of the expression of ICAM-1 at its mRNA and protein levels (Fig 3A, B). We next assessed ICAM-1 expression at the surface of neutrophils after the treatment with rmCIRP at various time-points and doses by flow cytometry. BMDN treated with rmCIRP at a constant dose 0.5 μg/ml significantly induced the surface expression of ICAM-1 by a mean value of 75% at 4 h, compared to PBS-treated cells (Fig 3C, D). Next, we sought to elucidate the dose-dependent effect of rmCIRP at a constant time 4 h for ICAM-1 expression on the surface of neutrophils. We found that the neutrophils treated with rmCIRP significantly induced ICAM-1 expression on their surface by mean values of 74% and 86% at doses 0.5 μg/ml and 1 μg/ml, respectively, as compared to PBS-treated cells (Fig 3E, F).

Treatment with rmCIRP induces ICAM-1 expression on neutrophils through TLR4-NF-κB-dependent pathway

We have previously shown that CIRP induces its pro-inflammatory function by binding to TLR4/MD2 complex in the macrophages [8]. ICAM-1 expression in the myeloid cells was shown to be governed by the activation of the transcription factor NF-κB [29]. We therefore assessed ICAM-1 expression on the neutrophils in rmCIRP-treated condition with or without neutralizing Ab for TLR4 and specific inhibitor for NF-κB. We noticed that the BMDN treated with rmCIRP dramatically induced ICAM-1 expression as compared to PBS-treated control. However, when BMDN were pre-treated with neutralizing Ab against TLR4, the upregulation of ICAM-1 expression following rmCIRP treatment was significantly attenuated by a mean value of 25% as compared to the isotype IgG pre-treated cells (Fig 4A, B). On the other hand, the cells pre-treated with isotype IgG control did not show attenuation in the surface expression of ICAM-1 on neutrophils following rmCIRP treatment as compared to rmCIRP alone-treated condition (Fig 4A, B). Similarly, the BMDN pre-treated with NF-κB inhibitor showed significant reduction in the expression of surface ICAM-1 on the neutrophils as compared to rmCIRP alone-treated cells, while there was no significant inhibition in ICAM-1 expression on the surface of the BMDN in vehicle (DMSO)-pre-treated condition (Fig 4C, D). Collectively, these data clearly suggest that rmCIRP-mediated ICAM-1 expression on the surface of neutrophils occurred through TLR4 and NF-κB-mediated pathway.

ICAM-1+ neutrophils express higher levels of iNOS and NETs in vitro

We next aimed to characterize ICAM-1 expressing neutrophils in terms of their iNOS expression. iNOS is expressed following induction by LPS, and serves as an inflammatory mediator [30, 31]. iNOS expression is associated with several inflammatory processes involving the lung that occurs during sepsis [30, 32]. In vitro treatment of BMDN with rmCIRP showed significant upregulation of iNOS expression in ICAM-1+ neutrophils as compared to ICAM-1− neutrophils (Fig 5A, B). Neutrophils often form NETs to kill bacteria [33]. However, in acute inflammatory disorders, aberrantly enhanced NETs formation and/or decreased NETs degradation may play key roles in initiation and perpetuation of

inflammatory responses and organ damage [15]. We therefore focused on the assessment of NETs by the ICAM-1$^+$ neutrophils. As shown in Fig 5C, D, following treatment with rmCIRP, the ICAM-1$^+$ BMDN showed significantly higher levels of extracellular MPO compared to ICAM-1$^-$ neutrophils. Surface-bound extracellular MPO serves as a pivotal marker of NETs.

ICAM-1$^+$ neutrophils in the lungs express increased levels of iNOS and NETs during sepsis

We next assessed iNOS and NETs measured by extracellular MPO in the ICAM-1$^+$ neutrophils of lungs in sepsis. We found significant upregulation of iNOS expression in ICAM-1$^+$ neutrophils compared to ICAM-1$^-$ neutrophils in the lung tissues following sepsis (Fig 6A, B). Similarly, we also found significant upregulation of surface bound MPO in ICAM-1$^+$ neutrophils compared to ICAM-1$^-$ neutrophils in the lungs during sepsis (Fig 6C, D).

ICAM-1 and NETs co-localize on neutrophils

Using fluorescent microscope we found that NETs as assessed by SYTOX green dye were co-localized with ICAM-1 on the surface of BMDN-treated with rmCIRP (Fig 7A).Using flow cytometry image stream tool, we further confirmed that ICAM-1 clearly co-localized with extracellular MPO, a component of NETs at the surface of neutrophils treated with rmCIRP (Fig 7B). On the other hand, the ICAM-1$^-$ neutrophils showed comparably reduced levels of NETs as shown by the surface levels of MPO (Fig 7B).

Deficiency of CIRP improves the survival of mice with sepsis

Sepsis was induced in WT and CIRP$^{-/-}$ mice by CLP, and the survival of mice was monitored for 10 days. We found that CIRP$^{-/-}$ mice showed a significant improvement in their survival outcome (78% survival) over that of WT mice (48% survival) at 10 day of CLP (Fig 8). Therefore, targeting CIRP could be an effective therapeutic tool for the management of sepsis.

DISCUSSION

The pro-inflammatory role of CIRP in macrophages, lymphocytes and ECs during sepsis has been demonstrated in the previous studies [8–11]. CIRP upregulates TNF-α production in macrophages and activates CD4$^+$ T lymphocytes by binding to its receptor TLR4/MD2 complex [8, 9]. CIRP also causes EC dysfunction by increasing inflammasome-mediated pyroptosis in sepsis [8, 9, 11]. It has recently been shown that CIRP induces lung endoplasmic reticulum (ER) stress and its associated downstream responses to promote sepsis-associated ALI [10].

Neutrophils, one of the major cell populations of innate-immune system play a pivotal role in host defense against pathogens [34]. Depletion of neutrophils frequently leads to a fatal complication, while excessive activation of neutrophils results in host tissue damage [35]. The protective and harmful effects of neutrophils depend on the stages of sepsis, as at the onset of sepsis neutrophils are important in attenuating bacteremia, whereas at the late onset of sepsis prolonged and excessive infiltration of neutrophils often cause organ dysfunction

ICAM-1 expression on neutrophils through the involvement of TLR4-dependent NF-κB-mediated canonical signal transduction pathway.

Aside from enhancing the effector functions by increasing ROS production and phagocytosis [25], the ICAM-1+ neutrophils were also shown to cause neutrophil aggregation and clumping in the microcirculation during systemic inflammatory response syndrome through the interaction between ICAM-1 and CD11b/CD18 receptors [24]. However, in murine model of polymicrobial sepsis, debilitating role of ICAM-1+ neutrophils in terms of exaggerating inflammation and injury has not been demonstrated. Here, we established an association between increased CIRP expression and ICAM-1+ neutrophils in lungs. Since CIRP was previously shown to cause ARDS during sepsis [10, 11], it is therefore exciting to know if ICAM-1+ neutrophils play pro-inflammatory role. We found that CIRP-treated neutrophils upregulated ICAM-1 expression which produced increased levels of iNOS. Excessive expression of iNOS leading to NO production to cause tissue injury and multiple organ dysfunction in sepsis has been reported [46], thereby implicating a possible deleterious role of ICAM-1+ neutrophils in lungs during sepsis.

The role of NETs in sepsis has just begun to explore. NETs are considered to be the double-edged swords of innate immunity. Although NETs represent an important strategy to immobilize and kill invading microorganisms, exaggerated NETosis increases risk of autoreactivity to NET components evident in sterile and non-sterile inflammatory disease [15, 47]. DNA, histones and MPO represent the major NET constituents [33]. We identified increased levels of MPO within ICAM-1+ populations of CIRP-treated neutrophils *in vitro*. Since we did not permeabilize cells while detecting MPO within neutrophils (Ly6G+ cells), thus these molecules were considered to be located outside the neutrophils, thereby confirming NET criteria. NETs can be defined as conventional late suicidal NETosis, a distinct form of active cell death and an early vital NETosis, a non-suicidal form which allows NET release from neutrophils staying viable [48]. Our current study although did not clearly define which form of NETs were predominant in ICAM-1+ neutrophils, nonetheless our present study guides us to design future experiments to identify the types of NETs in ICAM-1+ neutrophils, thereby providing novel insights on the pathophysiology of sepsis. Since NETs were previously shown to be detrimental in sterile inflammation [47], future studies for elucidation of the role of CIRP on ICAM-1+ neutrophils in sterile inflammation such as organ ischemia and reperfusion models and their subsequent association with NETs would be of great interest in revealing disease pathophysiology and the development of novel therapeutic strategies.

Previously, it has been shown that during inflammation a small population of neutrophils may acquire ICAM-1+ (CD54+) phenotype to facilitate their reverse transendothelial migration (rTEM) from tissues back to the vascular lumen [49, 50]. Although our study did not confirm whether or not these CIRP-induced ICAM-1 expressing neutrophils had rTEM property in sepsis, we demonstrated a novel function of these neutrophils for inducing NETs and iNOS production during inflammation. Further study to establish the association between CIRP-induced ICAM-1+ neutrophils and rTEM phenomenon will provide additional views on the function of these cells during sepsis. In human, ICAM-1+ neutrophils exist, but their functions remain elusive. Upregulation of CIRP and ICAM-1+

cells in human patients with septicemia have been reported in two different studies [8, 24], which therefore implicates a possible interaction between CIRP and ICAM-1$^+$ neutrophils to cause detrimental effect in sepsis.

In summary, we identified a novel function of CIRP to generate an immunologically active distinct phenotype of neutrophils (ICAM-1$^+$Ly6G$^+$) in blood and lungs during sepsis and under *in vitro* conditions. We also deduced CIRP directly increased the frequencies and numbers of ICAM-1$^+$ neutrophils through TLR4/NF-κB-mediated pathway. ICAM-1$^+$ neutrophils produced increased iNOS and NETs, thus might exaggerate inflammation and tissue injury during sepsis (Fig 9). Thus, targeting CIRP using knock-out mice showed reduced levels of ICAM-1$^+$ neutrophils in the lungs and finally provided an outstanding survival benefit in sepsis, implicating a novel therapeutic approach in sepsis-induced ARDS.

Acknowledgements

ABBREVIATIONS

|	
ALI	acute lung injury
ARDS	acute respiratory distress syndrome
CIRP	cold-inducible RNA-binding protein
CLP	cecal ligation and puncture
DAMPs	damage-associated molecular patterns
ICAM-1	intercellular adhesion molecule-1
IFN	interferon
IL	interleukin
iNOS	inducible nitric oxide synthase
LFA-1	leukocyte function-associated antigen-1
LPS	lipopolysaccharide
NETs	neutrophil extracellular traps
NF-κB	nuclear factor-κB
PAMPs	pathogen-associated molecular patterns
ROS	reactive oxygen species

| TLR4 | Toll-like receptor 4 |
| TNF | tumor necrosis factor |

REFERENCES

1. Singer M, Deutschman CS, Seymour CW, Shankar-Hari M, Annane D, Bauer M, Bellomo R, Bernard GR, Chiche JD, Coopersmith CM, Hotchkiss RS, Levy MM, Marshall JC, Martin GS, Opal SM, Rubenfeld GD, van der Poll T, Vincent JL, Angus DC (2016) The Third International Consensus Definitions for Sepsis and Septic Shock (Sepsis-3). JAMA 315, 801–10. [PubMed: 26903338]

2. Fleischmann C, Scherag A, Adhikari NK, Hartog CS, Tsaganos T, Schlattmann P, Angus DC, Reinhart K, Trialists I. F. o. A. C. (2016) Assessment of Global Incidence and Mortality of Hospital-treated Sepsis. Current Estimates and Limitations. Am J Respir Crit Care Med 193, 259–72. [PubMed: 26414292]

3. Rubenfeld GD, Caldwell E, Peabody E, Weaver J, Martin DP, Neff M, Stern EJ, Hudson LD (2005) Incidence and outcomes of acute lung injury. N Engl J Med 353, 1685–93. [PubMed: 16236739]

4. Han S and Mallampalli RK (2015) The acute respiratory distress syndrome: from mechanism to translation. J Immunol 194, 855–60. [PubMed: 25596299]

5. Kuipers MT, van der Poll T, Schultz MJ, Wieland CW (2011) Bench-to-bedside review: Damage-associated molecular patterns in the onset of ventilator-induced lung injury. Crit Care 15, 235. [PubMed: 22216838]

6. Aziz M, Jacob A, Yang WL, Matsuda A, Wang P (2013) Current trends in inflammatory and immunomodulatory mediators in sepsis. Journal of leukocyte biology 93, 329–42. [PubMed: 23136259]

7. Nishiyama H, Itoh K, Kaneko Y, Kishishita M, Yoshida O, Fujita J (1997) A glycine-rich RNA-binding protein mediating cold-inducible suppression of mammalian cell growth. J Cell Biol 137, 899–908. [PubMed: 9151692]

8. Qiang X, Yang WL, Wu R, Zhou M, Jacob A, Dong W, Kuncewitch M, Ji Y, Yang H, Wang H, Fujita J, Nicastro J, Coppa GF, Tracey KJ, Wang P (2013) Cold-inducible RNA-binding protein (CIRP) triggers inflammatory responses in hemorrhagic shock and sepsis. Nat Med 19, 1489–95. [PubMed: 24097189]

9. Bolognese AC, Sharma A, Yang WL, Nicastro J, Coppa GF, Wang P (2016) Cold-inducible RNA-binding protein activates splenic T cells during sepsis in a TLR4-dependent manner. Cell Mol Immunol

10. Khan MM, Yang WL, Brenner M, Bolognese AC, Wang P (2017) Cold-inducible RNA-binding protein (CIRP) causes sepsis-associated acute lung injury via induction of endoplasmic reticulum stress. Sci Rep 7, 41363. [PubMed: 28128330]

11. Yang WL, Sharma A, Wang Z, Li Z, Fan J, Wang P (2016) Cold-inducible RNA-binding protein causes endothelial dysfunction via activation of Nlrp3 inflammasome. Sci Rep 6, 26571. [PubMed: 27217302]

12. Amulic B, Cazalet C, Hayes GL, Metzler KD, Zychlinsky A (2012) Neutrophil function: from mechanisms to disease. Annu Rev Immunol 30, 459–89. [PubMed: 22224774]

13. Mantovani A, Cassatella MA, Costantini C, Jaillon S (2011) Neutrophils in the activation and regulation of innate and adaptive immunity. Nat Rev Immunol 11, 519–31. [PubMed: 21785456]

14. Branzk N and Papayannopoulos V (2013) Molecular mechanisms regulating NETosis in infection and disease. Semin Immunopathol 35, 513–30. [PubMed: 23732507]

15. Kaplan MJ and Radic M (2012) Neutrophil extracellular traps: double-edged swords of innate immunity. J Immunol 189, 2689–95. [PubMed: 22956760]

16. Staunton DE, Marlin SD, Stratowa C, Dustin ML, Springer TA (1988) Primary structure of ICAM-1 demonstrates interaction between members of the immunoglobulin and integrin supergene families. Cell 52, 925–33. [PubMed: 3349522]

17. Hubbard AK and Rothlein R (2000) Intercellular adhesion molecule-1 (ICAM-1) expression and cell signaling cascades. Free Radic Biol Med 28, 1379–86. [PubMed: 10924857]

18. Roy J, Audette M, Tremblay MJ (2001) Intercellular adhesion molecule-1 (ICAM-1) gene expression in human T cells is regulated by phosphotyrosyl phosphatase activity. Involvement of NF-kappaB, Ets, and palindromic interferon-gamma-responsive element-binding sites. J Biol Chem 276, 14553–61. [PubMed: 11278281]

19. Madjdpour C, Oertli B, Ziegler U, Bonvini JM, Pasch T, Beck-Schimmer B (2000) Lipopolysaccharide induces functional ICAM-1 expression in rat alveolar epithelial cells in vitro. Am J Physiol Lung Cell Mol Physiol 278, L572–9. [PubMed: 10710530]

20. Springer TA (1990) Adhesion receptors of the immune system. Nature 346, 425–34. [PubMed: 1974032]

21. Vestweber D (2008) VE-cadherin: the major endothelial adhesion molecule controlling cellular junctions and blood vessel formation. Arterioscler Thromb Vasc Biol 28, 223–32. [PubMed: 18162609]

22. Ding ZM, Babensee JE, Simon SI, Lu H, Perrard JL, Bullard DC, Dai XY, Bromley SK, Dustin ML, Entman ML, Smith CW, Ballantyne CM (1999) Relative contribution of LFA-1 and Mac-1 to neutrophil adhesion and migration. J Immunol 163, 5029–38. [PubMed: 10528208]

23. Dustin ML, Garcia-Aguilar J, Hibbs ML, Larson RS, Stacker SA, Staunton DE, Wardlaw AJ, Springer TA (1989) Structure and regulation of the leukocyte adhesion receptor LFA-1 and its counterreceptors, ICAM-1 and ICAM-2. Cold Spring Harb Symp Quant Biol 54 Pt 2, 753–65. [PubMed: 2577025]

24. Wang JH, Sexton DM, Redmond HP, Watson RW, Croke DT, Bouchier-Hayes D (1997) Intercellular adhesion molecule-1 (ICAM-1) is expressed on human neutrophils and is essential for neutrophil adherence and aggregation. Shock 8, 357–61. [PubMed: 9361346]

25. Woodfin A, Beyrau M, Voisin MB, Ma B, Whiteford JR, Hordijk PL, Hogg N, Nourshargh S (2016) ICAM-1-expressing neutrophils exhibit enhanced effector functions in murine models of endotoxemia. Blood 127, 898–907. [PubMed: 26647392]

26. Aziz M, Yang WL, Matsuo S, Sharma A, Zhou M, Wang P (2014) Upregulation of GRAIL is associated with impaired CD4 T cell proliferation in sepsis. J Immunol 192, 2305–14. [PubMed: 24477910]

27. Rasband WS ImageJ, U. S. National Institutes of Health, Bethesda, Maryland, USA, https://imagej.nih.gov/ij/, 1997–2016.

28. Zhou Y, Dong H, Zhong Y, Huang J, Lv J, Li J (2015) The Cold-Inducible RNA-Binding Protein (CIRP) Level in Peripheral Blood Predicts Sepsis Outcome. PLoS One 10, e0137721. [PubMed: 26361390]

29. Ruetten H, Thiemermann C, Perretti M (1999) Upregulation of ICAM-1 expression on J774.2 macrophages by endotoxin involves activation of NF-kappaB but not protein tyrosine kinase: comparison to induction of iNOS. Mediators Inflamm 8, 77–84. [PubMed: 10704144]

30. Hesse AK, Dörger M, Kupatt C, Krombach F (2004) Proinflammatory role of inducible nitric oxide synthase in acute hyperoxic lung injury. Respir Res 5, 11. [PubMed: 15377396]

31. Schulz C, Gillissen A, Schultze-Werninghaus G (1998) [Inducible nitric oxide synthase in pulmonary inflammatory processes]. Pneumologie 52, 340–9. [PubMed: 9715649]

32. Hollenberg SM, Broussard M, Osman J, Parrillo JE (2000) Increased microvascular reactivity and improved mortality in septic mice lacking inducible nitric oxide synthase. Circ Res 86, 774–8. [PubMed: 10764411]

33. Brinkmann V, Reichard U, Goosmann C, Fauler B, Uhlemann Y, Weiss DS, Weinrauch Y, Zychlinsky A (2004) Neutrophil extracellular traps kill bacteria. Science 303, 1532–5. [PubMed: 15001782]

34. Teng TS, Ji AL, Ji XY, Li YZ (2017) Neutrophils and Immunity: From Bactericidal Action to Being Conquered. J Immunol Res 2017, 9671604. [PubMed: 28299345]

35. Kolaczkowska E and Kubes P (2013) Neutrophil recruitment and function in health and inflammation. Nat Rev Immunol 13, 159–75. [PubMed: 23435331]

36. Hoesel LM, Neff TA, Neff SB, Younger JG, Olle EW, Gao H, Pianko MJ, Bernacki KD, Sarma JV, Ward PA (2005) Harmful and protective roles of neutrophils in sepsis. Shock 24, 40–7.

37. Camicia G, Pozner R, de Larrañaga G (2014) Neutrophil extracellular traps in sepsis. Shock 42, 286–94. [PubMed: 25004062]

38. Czaikoski PG, Mota JM, Nascimento DC, Sônego F, Castanheira FV, Melo PH, Scortegagna GT, Silva RL, Barroso-Sousa R, Souto FO, Pazin-Filho A, Figueiredo F, Alves-Filho JC, Cunha FQ (2016) Neutrophil Extracellular Traps Induce Organ Damage during Experimental and Clinical Sepsis. PLoS One 11, e0148142. [PubMed: 26849138]

39. Biron BM, Chung CS, O'Brien XM, Chen Y, Reichner JS, Ayala A (2017) Cl-Amidine Prevents Histone 3 Citrullination and Neutrophil Extracellular Trap Formation, and Improves Survival in a Murine Sepsis Model. J Innate Immun 9, 22–32. [PubMed: 27622642]

40. Nourshargh S and Alon R (2014) Leukocyte migration into inflamed tissues. Immunity 41, 694–707. [PubMed: 25517612]

41. Ley K, Laudanna C, Cybulsky MI, Nourshargh S (2007) Getting to the site of inflammation: the leukocyte adhesion cascade updated. Nat Rev Immunol 7, 678–89. [PubMed: 17717539]

42. Zhao YJ, Yi WJ, Wan XJ, Wang J, Tao TZ, Li JB, Wang JF, Deng XM (2014) Blockade of ICAM-1 improves the outcome of polymicrobial sepsis via modulating neutrophil migration and reversing immunosuppression. Mediators Inflamm 2014, 195290. [PubMed: 24891762]

43. de Oliveira S, Rosowski EE, Huttenlocher A (2016) Neutrophil migration in infection and wound repair: going forward in reverse. Nat Rev Immunol 16, 378–91. [PubMed: 27231052]

44. Gentile LF and Moldawer LL (2013) DAMPs, PAMPs, and the origins of SIRS in bacterial sepsis. Shock 39, 113–4. [PubMed: 23247128]

45. Melotti P, Nicolis E, Tamanini A, Rolfini R, Pavirani A, Cabrini G (2001) Activation of NF-kB mediates ICAM-1 induction in respiratory cells exposed to an adenovirus-derived vector. Gene Ther 8, 1436–42. [PubMed: 11571584]

46. Titheradge MA (1999) Nitric oxide in septic shock. Biochim Biophys Acta 1411, 437–55. [PubMed: 10320674]

47. Jorch SK and Kubes P (2017) An emerging role for neutrophil extracellular traps in noninfectious disease. Nat Med 23, 279–287. [PubMed: 28267716]

48. Yang H, Biermann MH, Brauner JM, Liu Y, Zhao Y, Herrmann M (2016) New Insights into Neutrophil Extracellular Traps: Mechanisms of Formation and Role in Inflammation. Front Immunol 7, 302. [PubMed: 27570525]

49. Buckley CD, Ross EA, McGettrick HM, Osborne CE, Haworth O, Schmutz C, Stone PC, Salmon M, Matharu NM, Vohra RK, Nash GB, Rainger GE (2006) Identification of a phenotypically and functionally distinct population of long-lived neutrophils in a model of reverse endothelial migration. J Leukoc Biol 79, 303–11. [PubMed: 16330528]

50. Hirano Y, Aziz M, Wang P (2016) Role of reverse transendothelial migration of neutrophils in inflammation. Biol Chem 397, 497–506. [PubMed: 26872312]
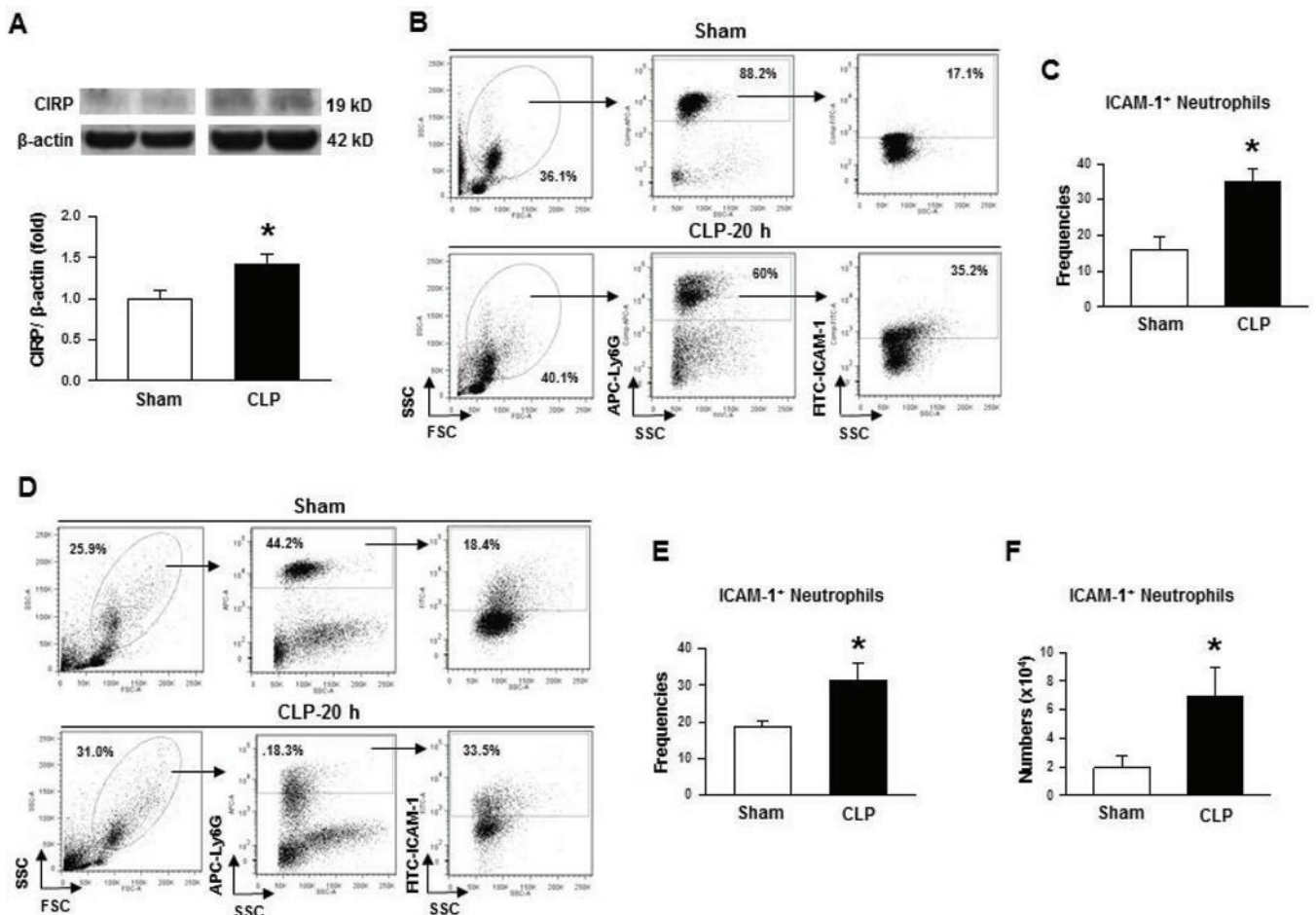
Figure 1: Status of CIRP levels and ICAM-1⁺ neutrophils in lungs during sepsis.
After 20 h of CLP or sham operation, lungs were harvested from mice. **(A)** Total protein was
extracted from lung tissues of each animal and CIRP expression at its protein level in lungs
was measured by Western blot. Each blot was quantified by densitometric analysis. CIRP
expression in each sample was normalized to β-actin expression and the mean value of sham
groups was standardized as one for comparison. Representative blots for CIRP and β-actin
from two independent experiments are shown. Data are expressed as means ± SE (n = 8–10
mice/group) and compared by *Student's t test* (*p < 0.05 vs. sham mice). **(B)** Whole blood
was collected from sham- and CLP-operated animals. A total of 250 μl of whole blood was
first treated with RBC lysis buffer and then after staining the cells with APC-Ly6G and
FITC-ICAM-1 (CD54) Abs flow cytometric detection was performed. A representative blot
indicating forward and side scatter, Ly6G and ICAM-1 (CD54) frequencies are shown. **(C)**
Bar diagram representing the mean frequencies of ICAM-1 expressing cells within Ly6G⁺
gated populations are shown. Data are expressed as means ± SE (n = 6 mice/group) and
compared by *Student's t test* (*p < 0.05 vs. sham mice). **(D)** Cells were isolated from lung
tissues by collagenase I digestion. After lysing red blood cells, the number of cells in each
sample was counted and a total of 1.5 × 10⁶ cells were reacted with APC-Ly6G and FITC-
ICAM-1 (CD54) Abs, followed by the assessment of cells using flow cytometry.
Representative dot blots indicating the frequencies of ICAM-1 expressing neutrophils as
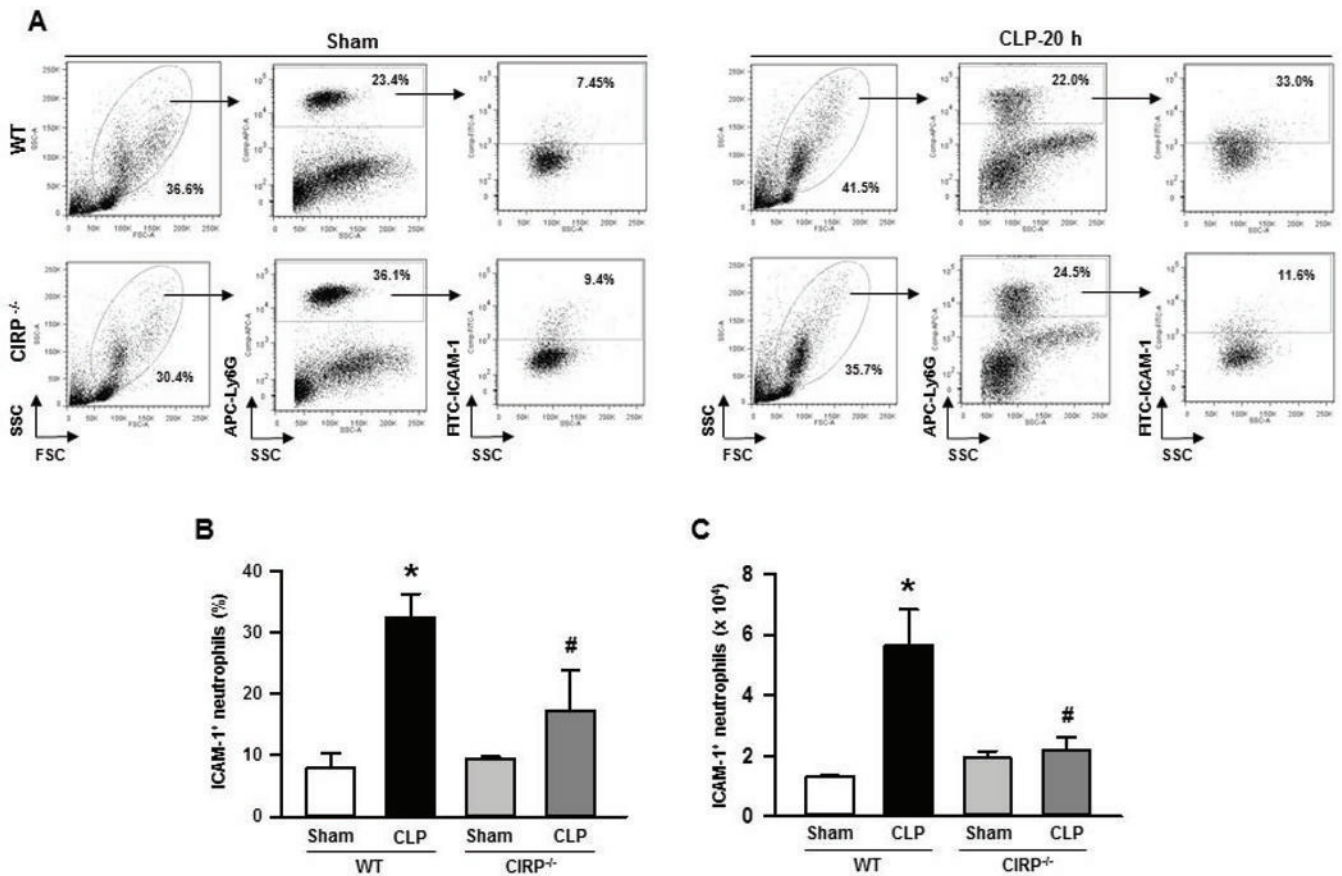
obtained from three independent experiments are shown. **(E)** Bar diagram representing the quantitative mean values of the frequencies of ICAM$^+$ neutrophils obtained from Ly6G$^+$ cells is shown. Data are expressed as means ± SE (n = 6 mice/group) and compared by *Student's t test* (*$p < 0.05$ vs. sham mice). **(F)** The total numbers of ICAM-1$^+$ neutrophils were determined by multiplying the ICAM$^+$ cells' frequencies from each sample with total number of cells in each lung. Bar diagram representing the mean values of the number of ICAM$^+$ neutrophils in each mouse is shown. Data are expressed as means ± SE (n = 6 mice/ group) and compared by *Student's t test* (*$p < 0.05$ vs. sham mice). CLP, cecal ligation and puncture; CIRP, cold-inducible RNA-binding protein; ICAM-1, intercellular adhesion molecule.

**Figure 2: Frequencies and numbers of ICAM-1^{+} neutrophils in lungs from WT and CIRP$^{-/-}$ mice during sepsis.**

At 20 h of sham or CLP operation, lungs were harvested from WT and CIRP$^{-/-}$ mice. ICAM-1 expression in neutrophils from lung cell lysates was detected by flow cytometry by reacting the cells with APC-Ly6G and FITC-ICAM-1 (CD54) Abs. **(A)** Representative dot blots of the frequencies of ICAM-1^{+} neutrophils in lungs from WT and CIRP$^{-/-}$ mice generated from three independent experiments are shown. Diagrammatic presentation of the quantitative mean values of the **(B)** frequencies and **(C)** numbers of ICAM-1^{+} neutrophils in lungs from WT and CIRP$^{-/-}$ mice are shown. Data are expressed as means ± SE (n = 3–5 mice/group) and compared by one-way ANOVA and SNK method (*$p < 0.05$ vs. WT sham; #$p < 0.05$ vs. WT CLP). CLP, cecal ligation and puncture; CIRP, cold-inducible RNA-binding protein; ICAM-1, intercellular adhesion molecule.
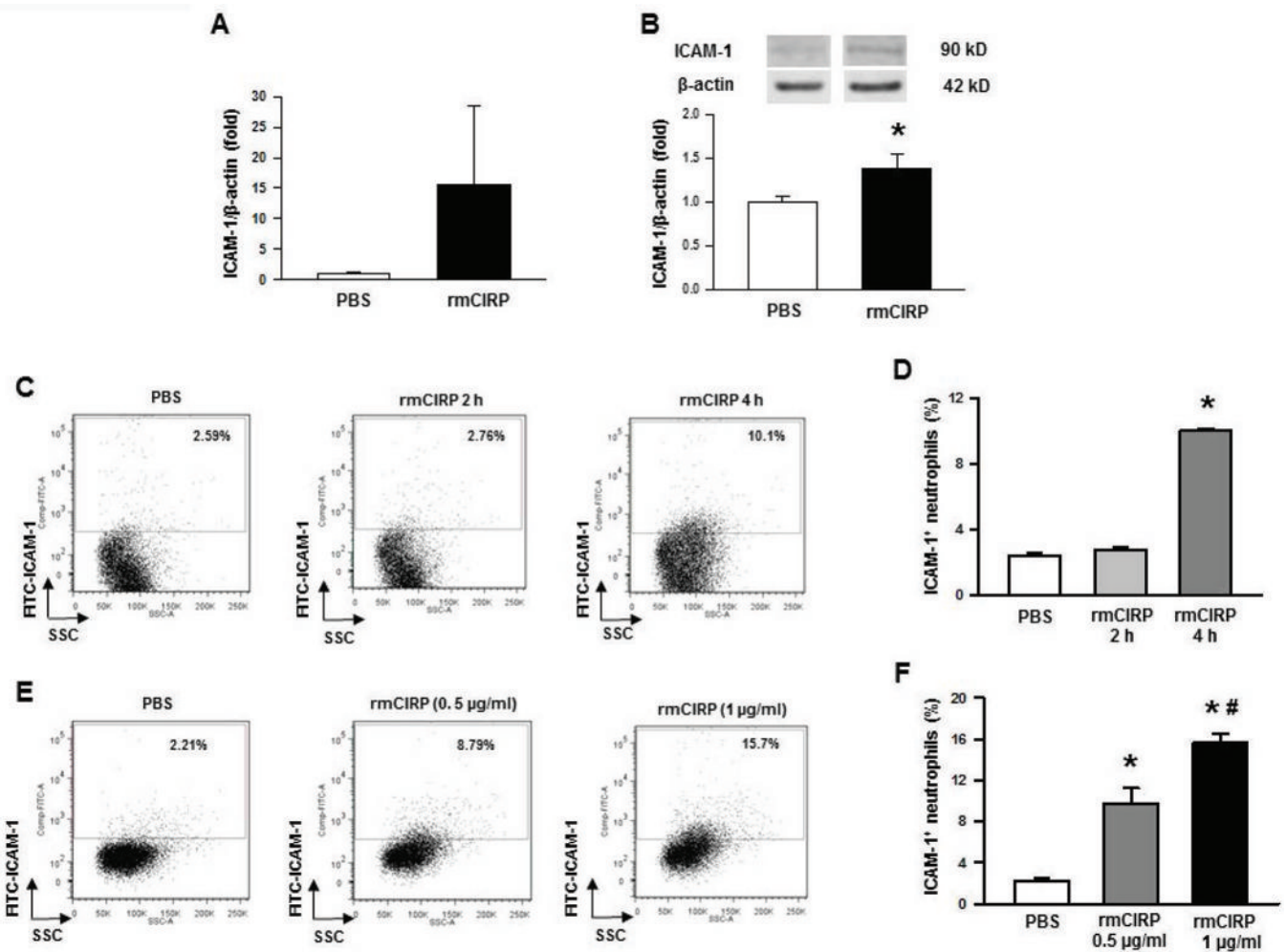
Figure 3: Assessment of ICAM-1 expression in BMDN treated with recombinant mouse CIRP *in vitro*.

Bone marrows were extracted from tibia and femoral bones of WT mice and BMDN were purified using magnetic beads. **(A)** A total of 2×10^6 BMDN were treated with rmCIRP (1 µg/ml) for 2 h and then assessed the mRNA levels of ICAM-1 by using real-time PCR. Data are expressed as means ± SE (n = 10 mice/group) and compared by *Student's t test.* **(B)** A total of 2×10^6 BMDN were treated with rmCIRP (1 µg/ml) for 4 h and then assessed the protein levels of ICAM-1 by using Western blot. Data are expressed as means ± SE (n = 7 mice/group) and compared by *Student's t test* (*p < 0.05 vs. sham mice). For the detection of surface levels of ICAM-1 expression, a total of 1×10^6 BMDN were stimulated with rmCIRP for various times and doses, followed by the assessment of BMDN by flow cytometry after staining them with APC-Ly6G and FITC-ICAM-1 Abs. **(C)** Dot blots and their **(D)** corresponding bar diagram representing the frequencies of ICAM-1^{+} cells within Ly6G^{+} populations following treatment of the BMDN with 0.5 µg/ml of CIRP at 2 h and 4 h time points. Data are expressed as means ± SE (n = 9/group) and compared by one-way ANOVA and SNK method (*p < 0.05 vs. PBS). **(E)** Dot blots and their **(F)** corresponding bar diagram representing the frequencies of ICAM-1^{+} cells within Ly6G^{+} populations following treatment of the BMDN with 0.5 and 1 µg/ml of CIRP for 4 h. Data are expressed
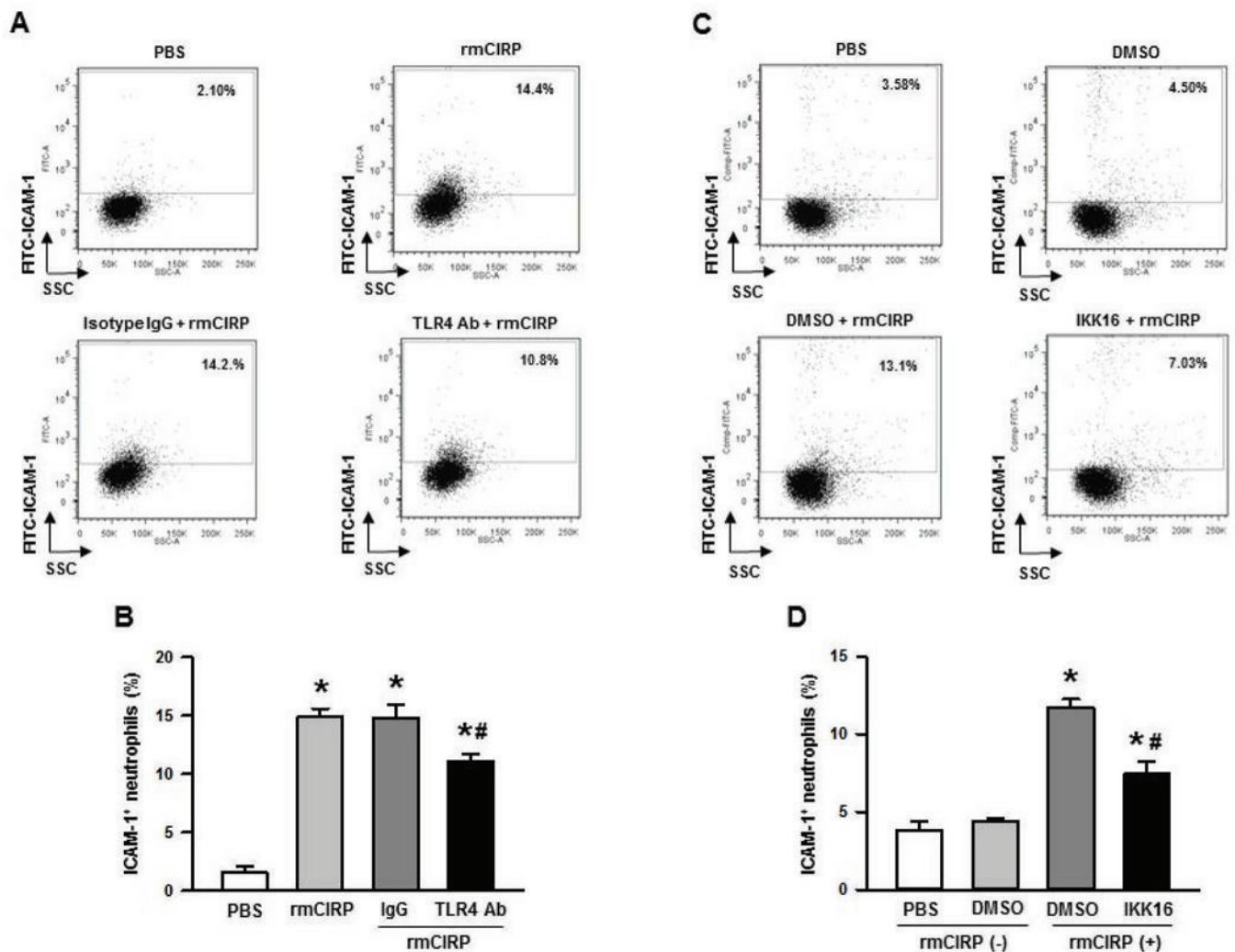
as means ± SE (n = 3/group) and compared by one-way ANOVA and SNK method (*p < 0.05 vs. PBS; #p < 0.05 vs. CIRP at 0.5 μg/ml dose). CIRP, cold-inducible RNA-binding protein; ICAM-1, intercellular adhesion molecule; rmCIRP, recombinant murine CIRP; BMDN, bone marrow-derived neutrophils.

Figure 4: Involvement of TLR4 and IκB pathways for rmCIRP-induced ICAM-1 expression in neutrophils.

(A, B) BMDN were purified and stimulated with 1 μg/ml of CIRP for 4 h at 37°C with 30 min prior incubating them with 6 μg/ml of anti-TLR4 neutralizing Ab or same dose of isotype IgG or **(C, D)** 0.5 μM of IKK16, a selective inhibitor of IκB kinase or DMSO as vehicle. After stimulation, BMDN were stained for the detection of surface ICAM-1 expression by flow cytometry. Representative dot blots and their corresponding bar diagrams indicating the frequencies of ICAM-1+ neutrophils are shown. Data are expressed as means ± SE (n = 9/group) obtained from three independent experiments and compared by one-way ANOVA and SNK method (*p < 0.05 vs. PBS; #p < 0.05 vs. isotype IgG or DMSO vehicle). CIRP, cold-inducible RNA-binding protein; ICAM-1, intercellular adhesion molecule; rmCIRP, recombinant murine CIRP; BMDN, bone marrow-derived neutrophils.
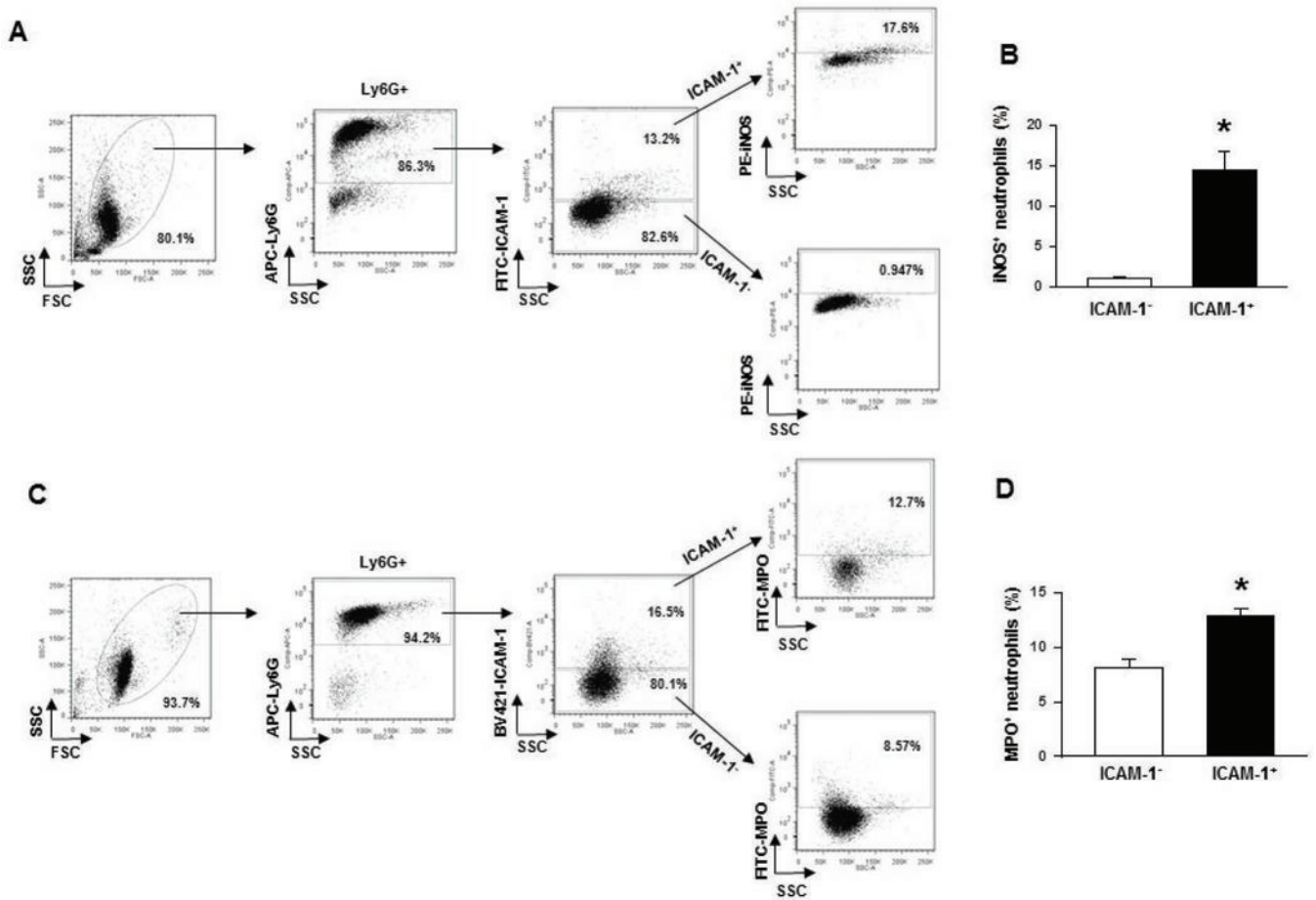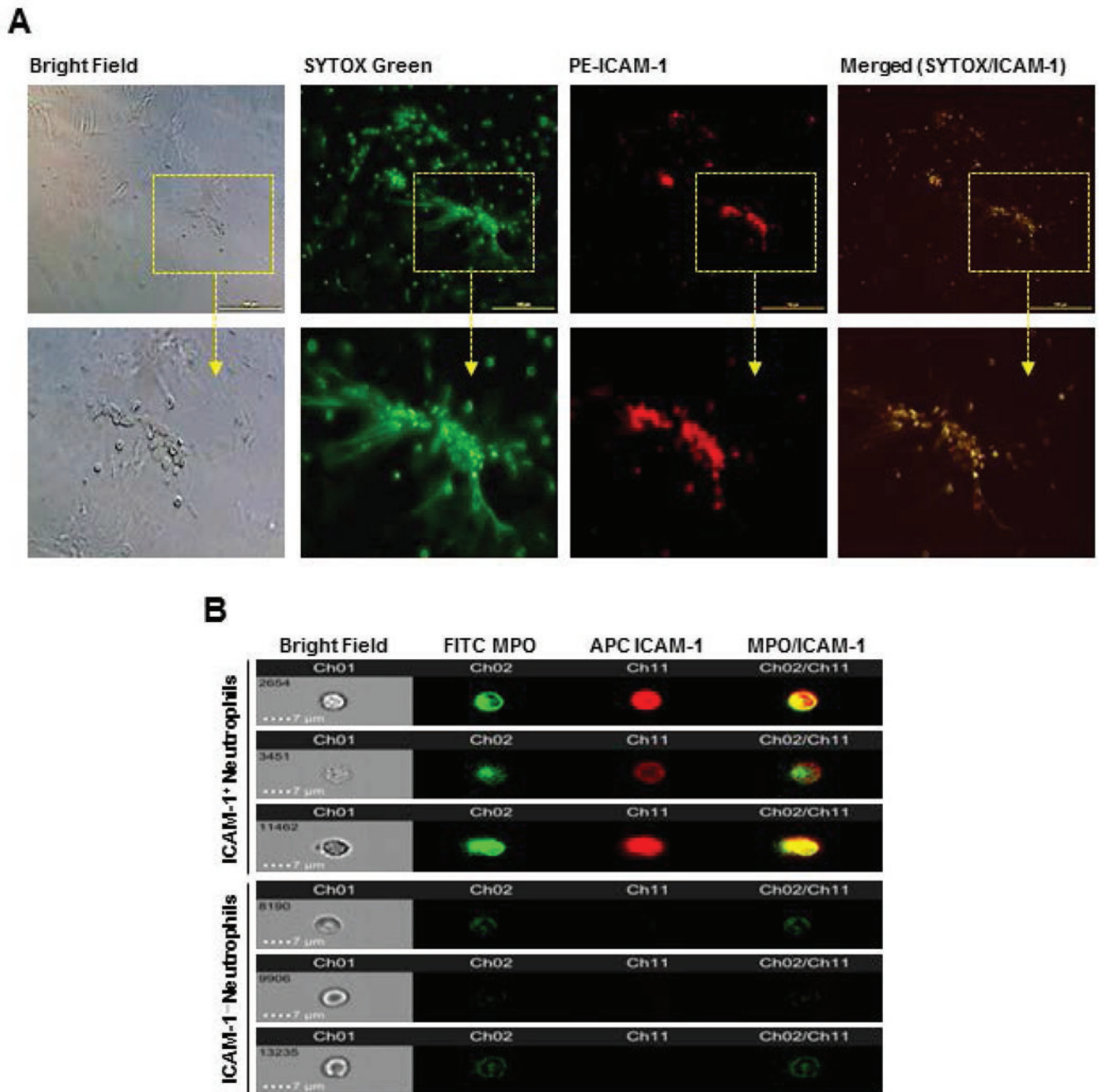
Figure 5: Assessment of iNOS and NETs in ICAM-1$^+$ neutrophils *in vitro*.
Purified BMDN (1×10^6 cells) were stimulated with 1 μg/ml of rmCIRP for 4 h. Surface ICAM-1 was stained with APC-Ly6G Ab and FITC-ICAM-1 Ab, followed by fixing and permeabilization steps, intracellular staining for iNOS expression was performed by using PE-anti-iNOS Ab. **(A, B)** Representative dot blots and corresponding bar diagram are shown. Data are expressed as means ± SE (n = 6 mice/group) and compared by *Student's t test* (*p < 0.05 vs. ICAM-1$^-$). In order to assess NETs *in vitro*, a total of 1×10^6 BMDN were stimulated with rmCIRP (1 μg/ml) at 37°C for 4 h. After fixing and blocking and without permeabilization of the cells, they were then stained with APC-Ly6G, BV421-ICAM-1 and FITC-MPO Abs. **(C, D)** Dot blots and corresponding bar diagram representing the frequencies of extracellular MPO in ICAM-1 expressing neutrophils are shown. Data are expressed as means ± SE (n = 4 mice/group) and compared by *Student's t test* (*p < 0.05 vs. ICAM-1$^-$). CIRP, cold-inducible RNA-binding protein; ICAM-1, intercellular adhesion molecule; rmCIRP, recombinant murine CIRP; BMDN, bone marrow-derived neutrophils.
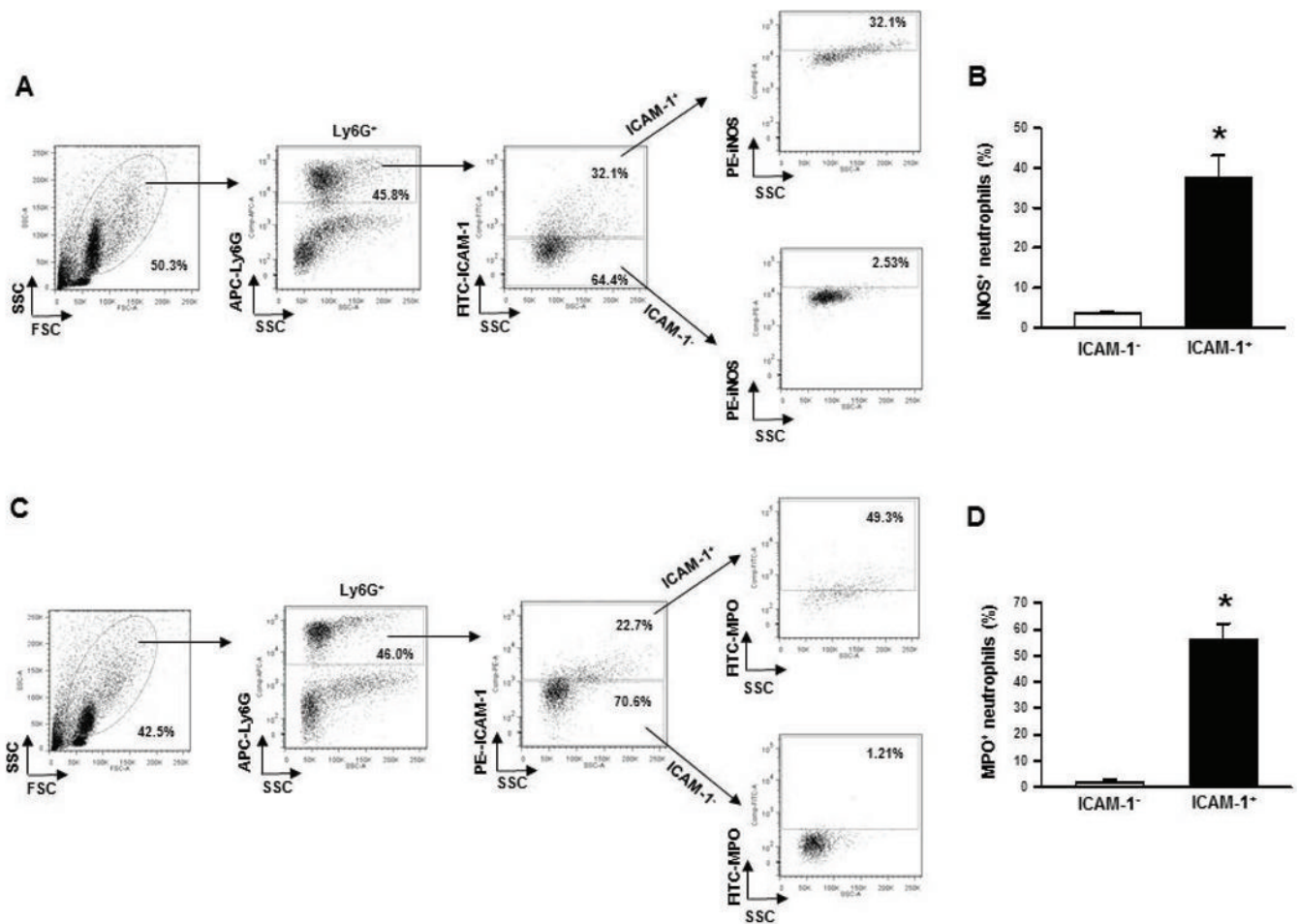
Figure 6: Assessment of iNOS and NETs in ICAM-1$^+$ neutrophils in lungs after sepsis.
At 20 h of sham or CLP operation, lungs were harvested from mice. iNOS and NETs were
detected in the single cell suspensions of lung tissues using flow cytometry by reacting the
cells with APC-Ly6G, FITC-ICAM-1 (CD54) and PE-iNOS Abs. **(A)** Representative dot
blots of the frequencies of iNOS expressing ICAM-1$^+$ neutrophils in lungs are shown. **(B)**
Diagrammatic presentation of the quantitative mean values of the frequencies of iNOS
expressing ICAM-1$^+$ neutrophils in lungs is shown. For the estimation of NETs, a total of 1
$\times 10^6$ cells isolated from the lung tissues of sham or 20 h after CLP operation were stained
with APC-Ly6G, PE-ICAM-1 (CD54) and FITC-MPO Abs and subjected to flow cytometry.
(C) Representative dot blots of the frequencies of extracellular MPO expressing ICAM-1$^+$
neutrophils in lungs are shown. **(D)** Diagrammatic presentation of the quantitative mean
values of the frequencies of extracellular MPO expressing ICAM-1$^+$ neutrophils in lungs is
shown. Data are expressed as means ± SE (n = 5 mice/group) and compared by *Student's t
test* (*p < 0.05 vs. ICAM-1$^-$). CLP, cecal ligation and puncture; ICAM-1, intercellular
adhesion molecule-1; MPO, myeloperoxidase; iNOS, inducible nitric oxide synthase.

A

Bright Field | SYTOX Green | PE-ICAM-1 | Merged (SYTOX/ICAM-1)

B

Bright Field | FITC MPO | APC ICAM-1 | MPO/ICAM-1

Figure 7: Co-localization of NETs in ICAM-1$^+$ neutrophils.
(**A**) A total of 1×10^5 BMDN grown in culture plate were stimulated with rmCIRP (1 μg/ml) for 4 h. Cells were stained with SYTOX Green and anti-mouse ICAM-1 Abs and assessed under florescence microscope. Representative images (selected from n = 10 random locations/well/group) showing the co-localization of NETs on ICAM-1$^+$ neutrophils are shown. (**B**) BMDN (2×10^6) were stimulated with 1 μg/ml rmCIRP for 4 h at 37°C. Cells were surface stained with FITC MPO and APC ICAM-1 Abs and analyzed using an ImageStreamX Mark II flow cytometer and INSPIRE and IDEAS software. Representative
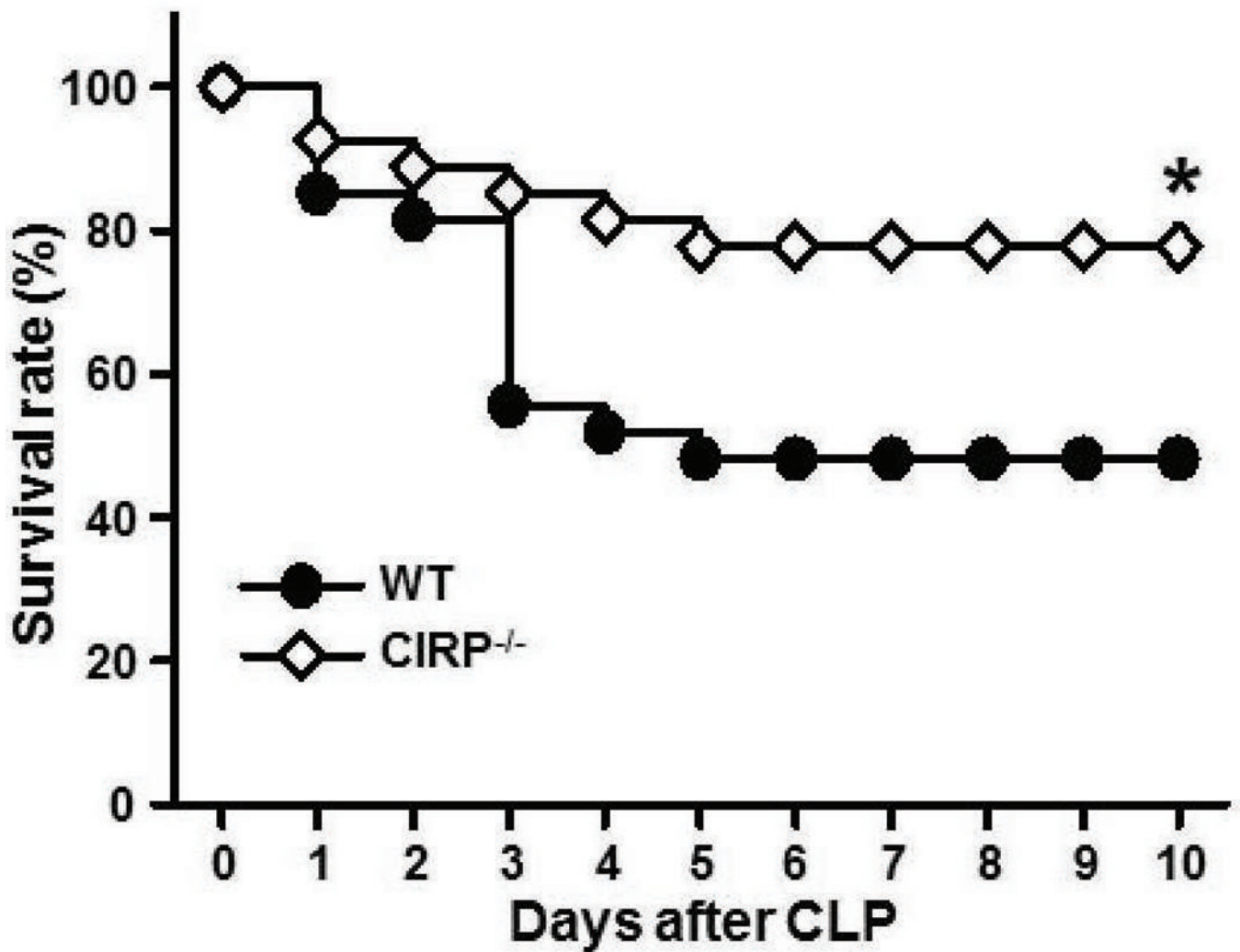
images (acquired from 10,000 events/group) showing the co-localization of NETs on ICAM-1$^+$ neutrophils are shown. BMDN, bone marrow-derived neutrophils; rmCIRP, recombinant murine CIRP; ICAM-1, intercellular adhesion molecule-1; MPO, myeloperoxidase;

Figure 8: Survival outcomes in WT and CIRP$^{-/-}$ mice in sepsis.
Sepsis was induced in WT and CIRP$^{-/-}$ mice by CLP as described in Materials and
Methods. A 10-day period Kaplan-Meier survival curve generated from WT and CIRP$^{-/-}$
mice (n = 27 mice/group) with CLP-induced sepsis is shown. *p<0.05 vs. WT CLP mice,
determined by the log-rank test. CLP, cecal ligation puncture; CIRP, cold-inducible RNA-
binding protein.
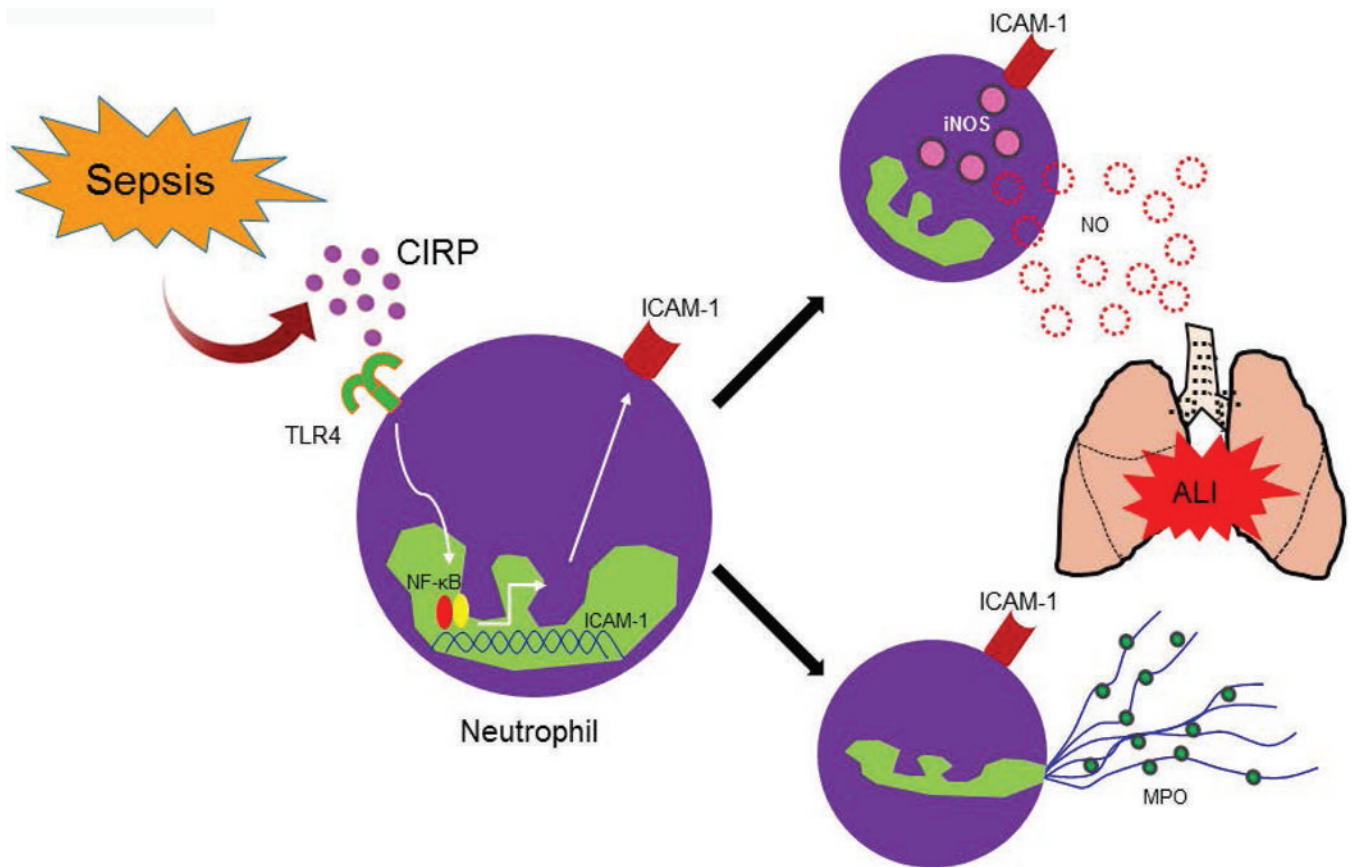
Figure 9: Summary of findings.
Bacterial sepsis causes upregulation of CIRP which binds to TLR4. CIRP-TLR4 interaction in neutrophils leads to upregulation of ICAM-1 expression through NF-κB pathway. Functionally, the ICAM-1^{+} neutrophils produce excessive iNOS and NETs and promote inflammation and injury to the tissues. CIRP, cold-inducible RNA-binding protein; TLR4, Toll-like receptor 4; NETs, neutrophil extracellular traps; iNOS, inducible nitric oxide synthase; ICAM-1, intercellular adhesion molecule-1; MPO, myeloperoxidase.